American Journal of Chemical Engineering
2018; 6(5): 107-120
http://www.sciencepublishinggroup.com/j/ajche
doi: 10.11648/j.ajche.20180605.15
ISSN: 2330-8605 (Print); ISSN: 2330-8613 (Online)

The Effect of Graphene/TIO_2 Nanomaterials on Photocatalytic Performance for Industrial Wastewater Treatment

Abd El-Aziz Hassanin Konsowa, Yehia Abd El-Qadeer EL-Taweel, Shahinaz Ibrahim Abogaliel

Department of Chemical Engineering, Alexandria University, Alexandria, Egypt

Email address:
akonsowa@alex-eng.edu.eg (A. El-Aziz H. Konsowa), ytawil20@gmail.com (Y. A. El-Qadeer EL-Taweel), eng_shahi_2010@yahoo.com (S. I. Abogaliel)

To cite this article:
Abd El-Aziz Hassanin Konsowa, Yehia Abd El-Qadeer EL-Taweel, Shahinaz Ibrahim Abogaliel. The Effect of Graphene/TIO_2 Nanomaterials on Photocatalytic Performance for Industrial Wastewater Treatment. *American Journal of Chemical Engineering*. Vol. 6, No. 5, 2018, pp. 107-120. doi: 10.11648/j.ajche.20180605.15

Received: September 5, 2018; **Accepted**: October 8, 2018; **Published**: November 6, 2018

Abstract: The aim of the present work is to combine TiO_2/Graphene to increase photo-catalytic activity and obtain efficient removal of direct red 23 azo dye without difficult synthesis. Many operating variables which affect the process and some design aspects were studied. Reactor geometry is the main design parameter where slurry rectangular reactor and bubble column were compared with respect to hydrodynamic regimes, overall degradation efficiency and applicability in industrial scale. The removal rate was found to increase with increase in TiO_2 concentration, approaching a limiting value at catalyst loads of 3g/L. For rectangular reactor only 0.005g/L of rGO able to enhance the activity of photo-catalysis. However, the optimum concentration of rGO is decreased in the bubble column reactor to be 0.001g/L. In both reactor systems, photocatalytic activity increase significantly by decreasing wavelength of the irradiated lamp from 365 nm to 254 nm. Also, results show the ability of bubble column reactor to treat high concentrations of dye up to 200 ppm. That makes it suitable to be integrated with biological system to convert non-biodegradable contaminates into biodegradable organics. That reduces the operating cost of the process and makes it more applicable in industrial scale. Rectangular reactor has the ability to be modified to use sunlight instead of artificial lamps because of high surface exposed to sunlight. In general the performance of bubble column reactor was better than rectangular reactor because it has excellent mass transfer characteristics, which enhance the efficiency of the process.

Keywords: Wastewater Treatment**,** Photocatalysis, Nanomaterials, Slurry Bubble Column Reactor

1. Introduction

Treatment of colored wastewater from textile or other industries is a serious problem that has attracted the attention of many researchers during last decades [1]. Textile industries produce large amounts of wastewater containing various dye pollutants and more than 60% of dyes used in these industries are azo dyes. Most of the azo dyes are non-biodegradable and their release into the environment poses a major threat to the surrounding eco systems [2]. Because of the increasing levels and complexity of polluted effluents, conventional wastewater treatment technologies are often not sufficient for the purification and disinfection of polluted waters [3]. Moreover processes such as gravity settling, filtration, air stripping, or adsorption to activated carbon are separation processes that leave a waste stream to be treated and disposed [4]. Photocatalysis could be one of the future alternatives because of its low costs and effectiveness. As energy source uses light (both solar and artificial), the applied catalysts are non-toxic (such as TiO_2) and the decomposition of the pollutants can be conducted until total mineralization (CO_2, water, ions) [5]. TiO_2 has been the most widely researched photocatalyst, but suffers from low efficiency and narrow light response range. Combining TiO_2 with carbonaceous nanomaterials is being increasingly investigated as a means to increase photocatalytic activity [6]. Industrial treatment of wastewater with various pollutants by photocatalytic oxidation with TiO_2 is

uncommon because of the fast recombination rate of the photo-induced electron–hole pairs in TiO_2 which reduces the efficiency of the photocatalytic reactions significantly, thus limiting its practical applications. Several strategies have been developed to enhance the photocatalytic efficiency of TiO_2 photocatalyst. Besides traditional doping, metal deposition, and coupling of composite semiconductors, the combination of carbon with TiO_2 was confirmed to be an effective way for separating electron–hole pairs. Up to now, a variety of TiO_2–carbon composites had been fabricated, such as TiO_2/carbon nanotube, TiO_2/C60, TiO_2/activated-carbon composites, and so on. The photocatalytic activity of these TiO_2/carbon composites was indeed improved to a certain extent [7, 8]. As a new member of the carbon family, graphene has attracted worldwide attention since it was discovered by Geim et al. in 2004 [9]. In recent years, the combination of TiO2 and graphene had been proved to be an effective pathway to improve the photocatalytic activity of TiO_2 due to the excellent adsorbability and conductivity of graphene [8].

In 2011, A series of graphene/titanate nanotubes (TNTs) photocatalysts using graphene and nanoscale TiO_2 or P25 as original materials were fabricated by hydrothermal method. Both low hydrothermal temperature and proper amount of graphene are propitious to better photoactivity. The photocatalytic activities of these nanocomposites far exceed that of P25 and pure TNTs [10]. In 2012, Khalid, et al prepared nitrogen doped TiO_2 nanoparticles decorated on graphene sheets by a low temperature hydrothermal method and demonstrated that GR-N/TiO_2 composites can effectively photodegrade MO, showing an impressive photocatalytic enhancement over pure TiO_2 [11]. There are various ways have been developed to prepare photocatalyst such as sol-gel method [12, 13], hydrothermal method [14], CVD [15] or electro-spinning [16]. Nevertheless, these methods have some disadvantages for industrial applications. For example, special apparatuses will be needed such as electro-spinning machine [17]. In 2014, Felix, et al studied using heterogeneous photocatalytic degradation of Naphthalene using Periwinkle Shell Ash (PSA) and effect of operating variables on the process. He found that the optimum values were obtained to be: contact time, 210 minutes; initial naphthalene concentration, 25 mg/L; PSA dosage, 2 g; pH, 9 [18]. According to literature, using GO as a starting material for preparing photocatalyst is demonstrated [8, 19-28]. Up to now, there are a scarce studies which emphasize on the fabrication of nanostructured TiO_2/graphene photocatalyst with efficient electron-hole separation ability with using graphene as a starting material. This present work is to combine TiO_2/Graphene by simple mixing to increase photo-catalytic activity and obtain efficient removal of direct red 23 azo dye without difficult synthesis. Sometimes, synthesis methods are expensive and time consuming. Many operating parameters (variables) which affect the process and some design aspects were studied and adjusted to maximize the process efficiency.

2. Materials and Methods

2.1. Materials

Commercial Anatase TiO_2 (98.48% Anatase) was obtained from EL KAYAR, Egypt. Reduced Graphene Oxide (rGO) was purchased from NanoTech Company, Egypt. Direct red 23 (Scarlet 4BS), Egypt. Other chemicals such as H_2O_2 (30%, w/v), $FeSO_4$, $AgNO_3$ and CuSO4, El-Gomhoria Company, Egypt.

2.2. Method

Figure 1: shows a schematic diagram of the present experimental setup. It mainly consists of two different photocatalytic configurations A) Plexi-glass rectangular photo-reactor (50*5*15 cm3), the height of the solution was 5 cm and tubular UV lamp (power 8W, ʎ=254 nm, and length 30 cm) was located 10 cm from the surface of the dye solution, the volume of the treated solution was 1L. Air pumps was used to flow the air into the reactor through air distributor to supply system with O_2 and provide sufficient mixing inside the photocatalytic system, B) Bubble column reactor (D=10 cm, H=50 cm), UV lamp (power 8W, ʎ= 365 nm, and length 30 cm) was immersed in the center of the bubble column and surrounded by a Pyrex glass tube which prevent UV lamp from damage inside the column, Pyrex glass allowed UV light with ʎ= 365 nm to pass through it [29]. Air was allowed to pass from air compressor to the bottom of the bubble column. The volume of the treated solution was 4L.

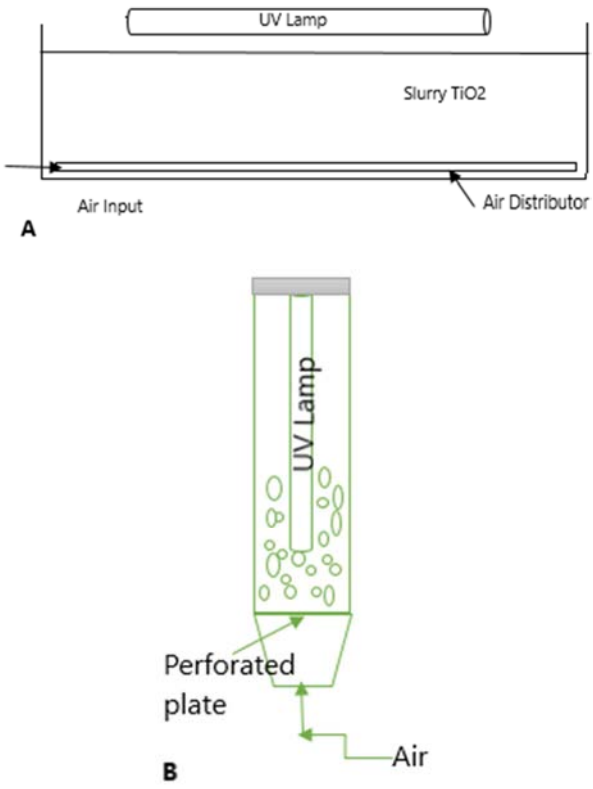

Figure 1. *A) Slurry Rectangular Reactor B) Slurry Bubble Column Reactor.*

3. Results and Discussion

3.1. Characterization of TiO_2

3.1.1. Scanning Electron Microscopy (SEM)

SEM images of Anatase TiO_2 in Figure 2: show the morphology and particle size of TiO_2. It is clear that TiO_2 particles are almost spherical with particle size about 100 nm. Also we can notice the tendency of TiO_2 for agglomeration.

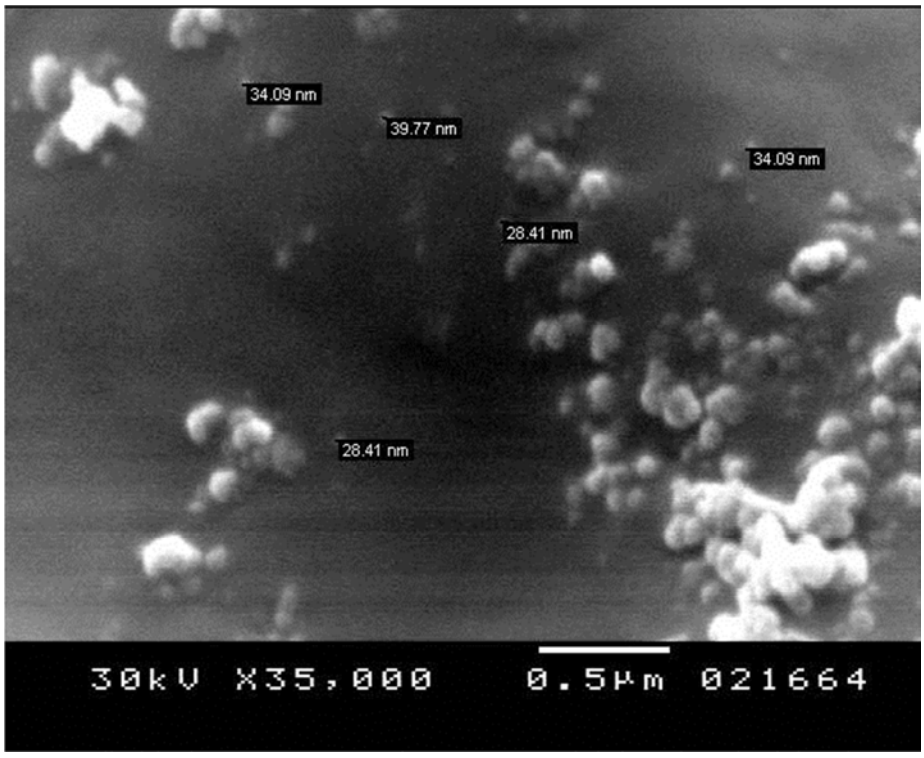

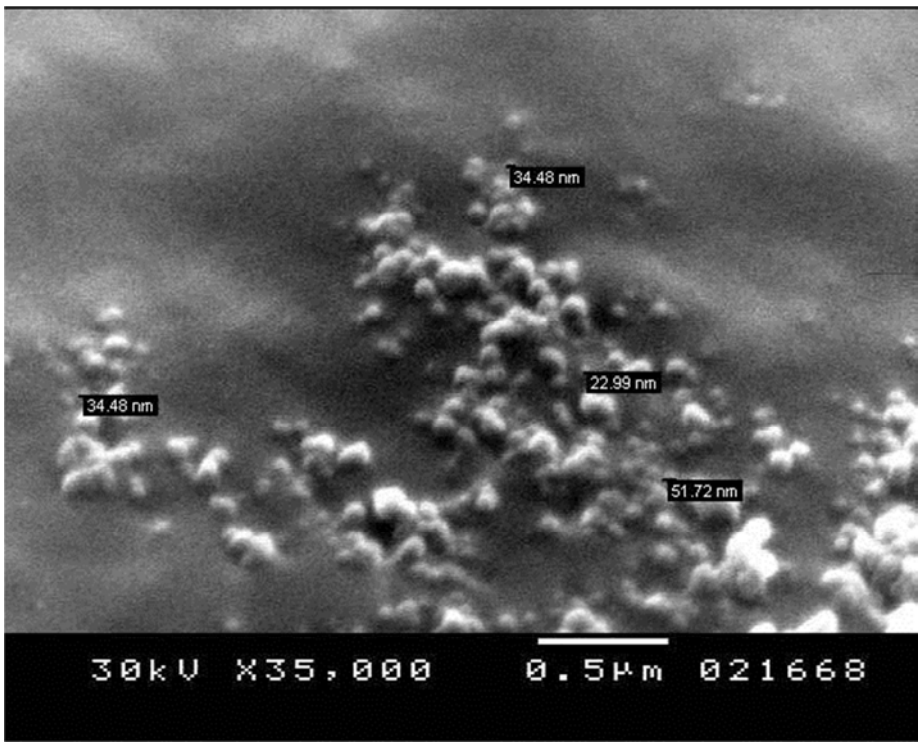

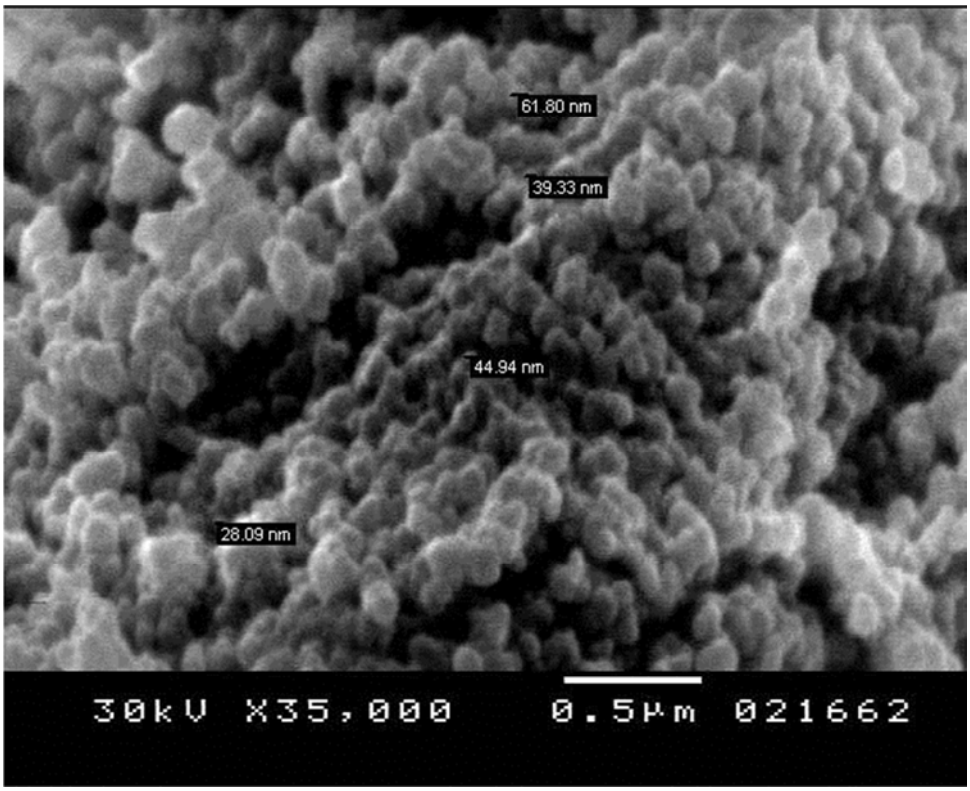

Figure 2. *SEM images of Anatase TiO_2.*

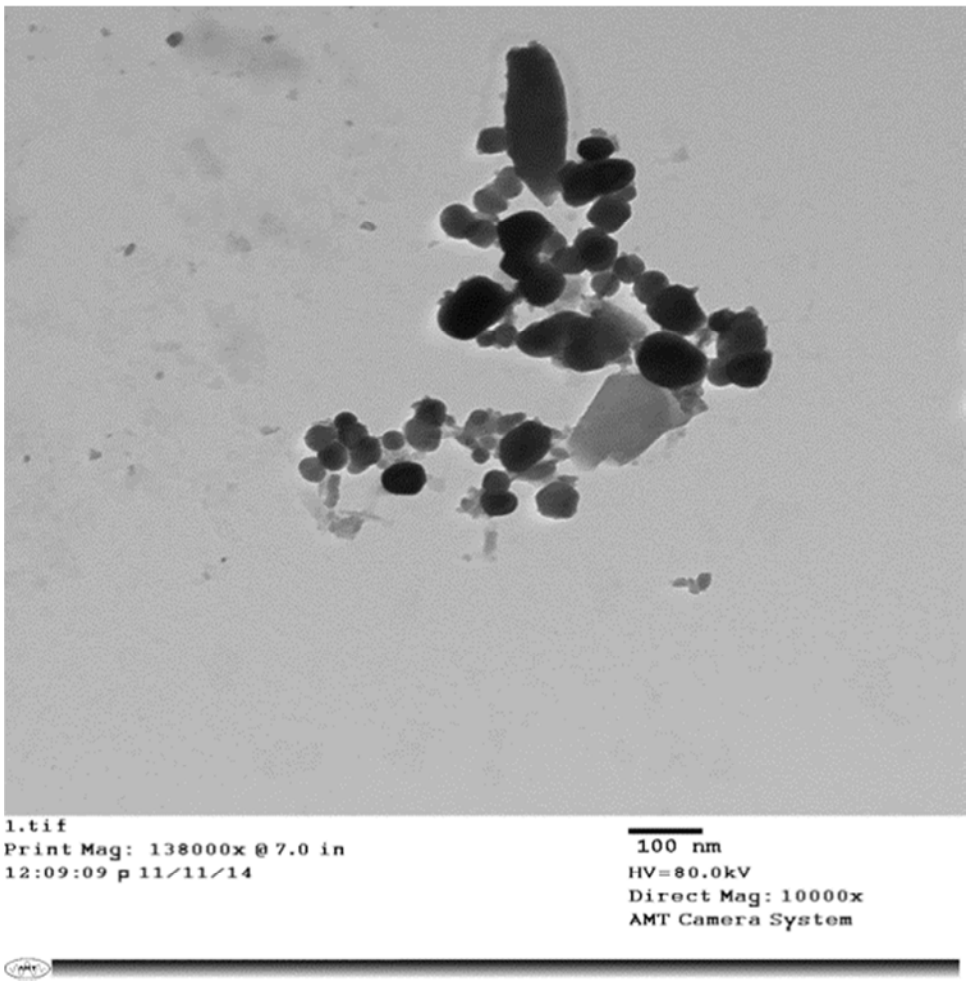

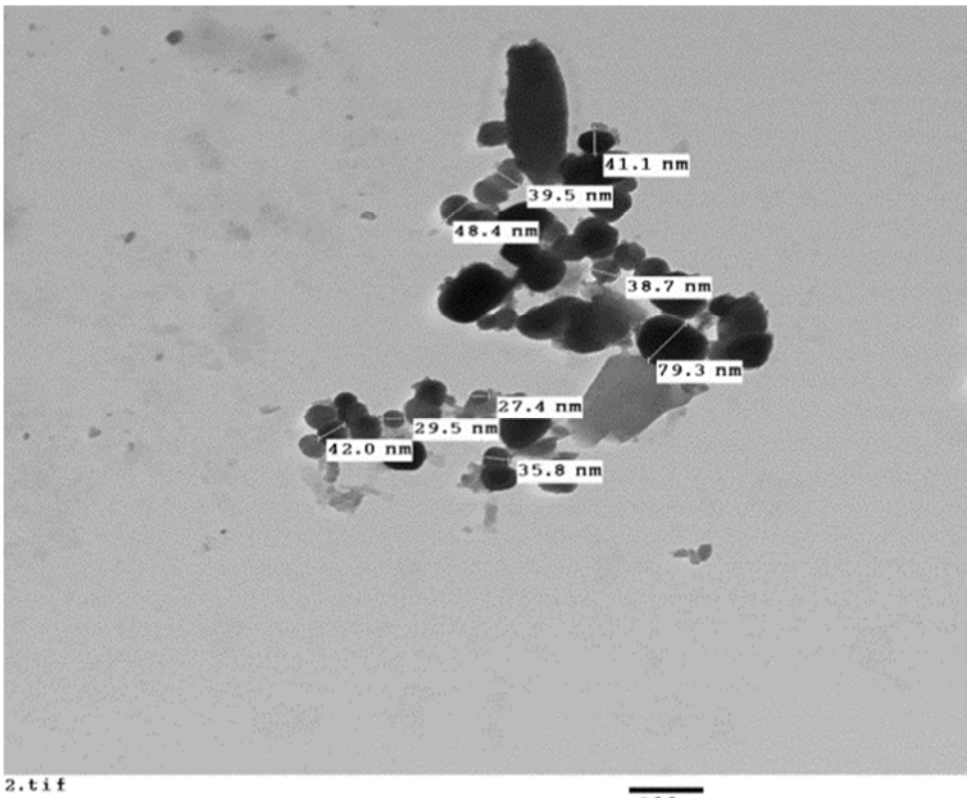

2.tif
Print Mag: 138000x @ 7.0 in
12:09:09 p 11/11/14

100 nm
HV=80.0kV
Direct Mag: 10000x
AMT Camera System

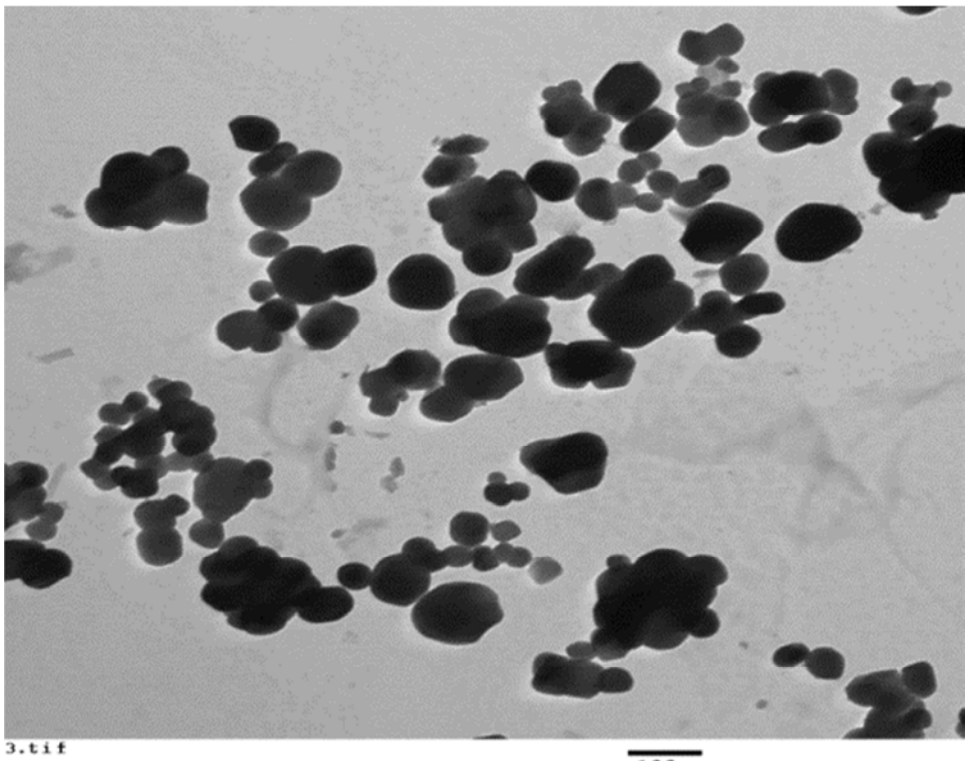

3.tif
Print Mag: 138000x @ 7.0 in
12:15:13 p 11/11/14

100 nm
HV=80.0kV
Direct Mag: 10000x
AMT Camera System

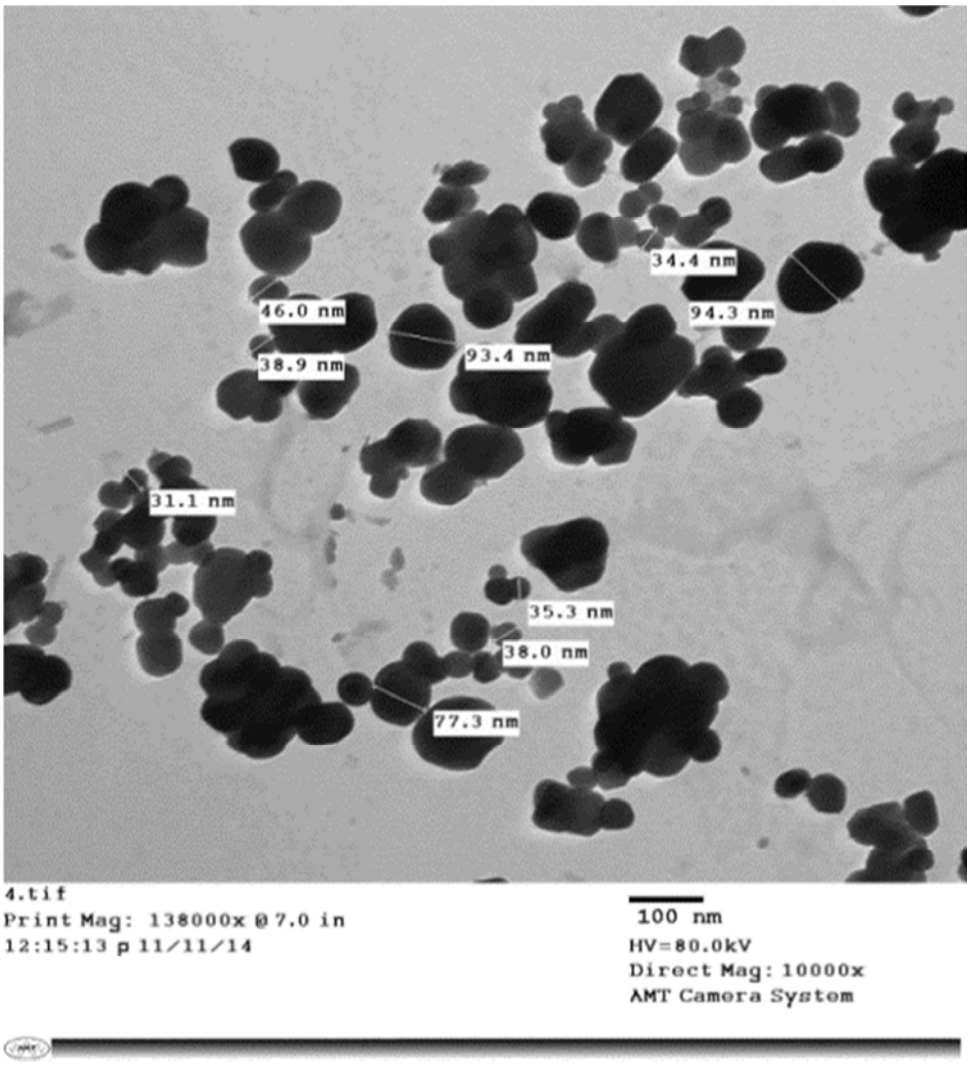

Figure 3. *TEM images of Anatase TiO_2.*

3.1.2. Transmission Electron Microscopy (TEM)

The results of SEM images can be confirmed by TEM analysis as shown in Figure 3. TEM images show that TiO_2 particles are spherical and oval with particle size below 100 nm. Size and shape of TiO_2 nanoparticle can affect the photo-catalytic degradation of direct red 23 (scarlet 4BS). As the particle size decrease the photo-catalytic activity increase, that can be attributed to two reasons. First: decreasing particle size reduces the electron–hole recombination due to reduced migration distances and fewer defects in route to surface reaction sites. Second: increasing surface area of TiO_2 particles lead to increase active sites on the TiO_2 which lead to increase adsorbability of direct red 23 dye on TiO_2 particles and thus, increasing the kinetics of the photocatalytic process. The same results were obtained by Xu et al. He found that adsorption rate and adsorbability of MB on suspended TiO_2 particles increased as the particle sizes decreased, photocatalytic activity also increased with the decrease in the TiO_2 particle size [30]. Also, the images show the regular spherical or oval shape for the TiO_2 nanoparticles which indicate high crystallinity of it.

3.2. The Effect of TiO_2 Loading

Figure 4: and Figure 5: show the effect of TiO_2 concentration on the rate of photo-catalytic degradation of azo dye (Scarlet 4BS) in rectangular reactor and bubble column reactor respectively. The removal rate was found to increase with increase in TiO_2 concentration, approaching a limiting value at catalyst loads of 3g/L. This can be attributed to increasing number of active sites for adsorption. However photo-catalytic activity decreases after reaching the limiting value due to the increase in solution opacity which leads to decrease in the penetration of the photons to TiO_2 surface. Juntima Chungsiriporn et al. found the same trend for de-colorization of rhodamine B (RB) and malachite green (MG) dye solutions (20 mg/L) in the presence of TiO_2 photo-catalyst and he explained the decreasing in Photo-catalytic degradation after the limiting value by the fact that high TiO_2 loadings tend to aggregate, which reduces the catalytic activities by reducing the specific surface area of the TiO_2 powder catalyst [31]. Also, Figure 5: represents the TiO_2 dose in the bubble column reactor. It is clear that 12 g of TiO_2 is the optimum dose to decolorize 4L of the dye solution.

3.3. Effect of rGO Dose

The photo-catalytic degradation increase by increasing rGO content in both rectangular and bubble column reactors. The effect of various concentrations of rGO from (0.002 - 0.02g) with constant amount of total mixture (TiO_2/rGO) is shown in this section.

For rectangular reactor, it is clear from figure 6: that only small concentration of rGO (0.005g/L) able to enhance the activity of photo-catalysis. That can be attributed to decrease e^-/h^+ recombination by trapping electrons from the conduction band of TiO_2 as well as increase surface area of the catalyst and adsorption capacity of the dye. A further increase in rGO content higher than 0.005g/L leads to decrease of the photo-catalytic activity because the excess loading of rGO would prevent the light from reaching the surface of the TiO_2. The same result was obtained for the bubble column reactor. However, the optimum concentration of rGO is decreased in the bubble column reactor to be (0.001g/L) and 0.004g to treat 4L of the dye solution as shown in figure 7:. Shaobin Wang and Jiaguo Yu studied the effect of rGO loading on photocatalytic degradation of methylene blue (MB) and acetone respectively, they found the same result [32, 8].

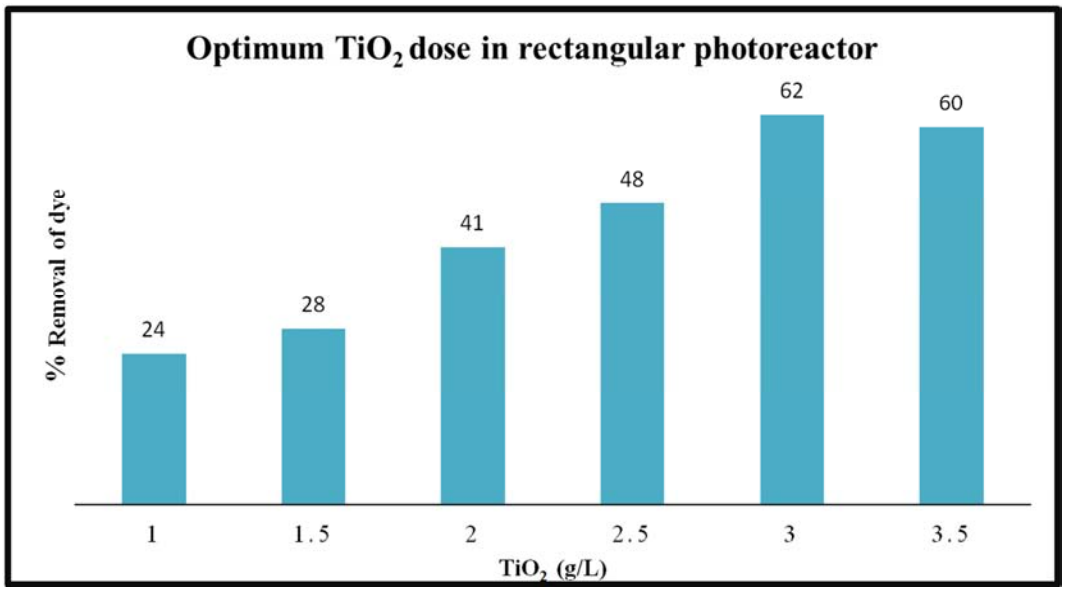

Figure 4. *Optimum TiO_2 dose for photo-catalytic degradation of direct red 23 in rectangular reactor. Initial concentration=50 mg L^{-1}, ʎ=254nm, Air flow-rate=10 L/min, 0.2%wt rGO and Contact time around 75 min.*

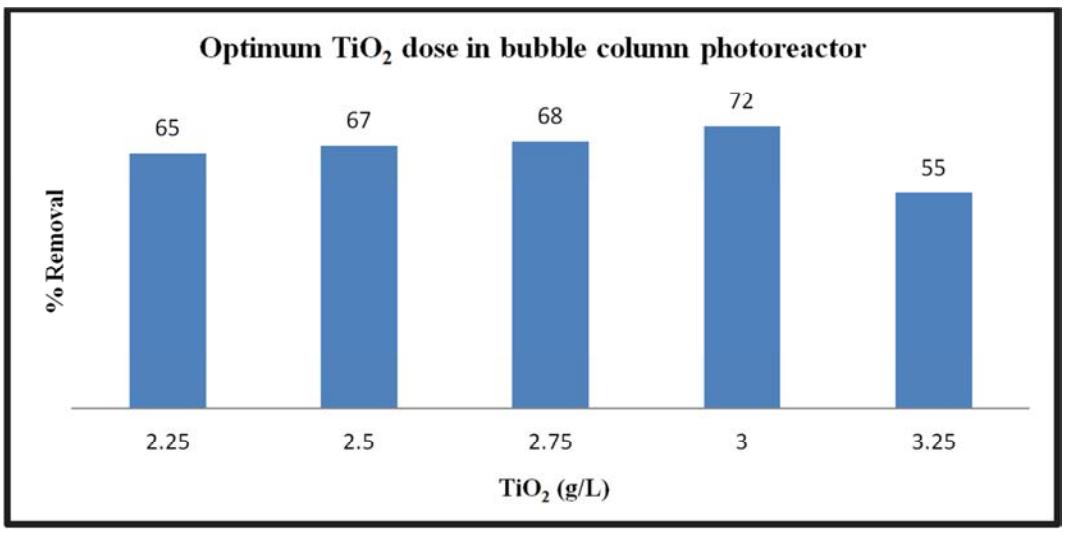

Figure 5. *Optimum TiO_2 dose for photocatalytic degradation of direct red 23 in bubble column reactor. Initial concentration=50 mg/L, ʎ=365nm, Volume of reactor 4L, Air flowrate=15 L/min, 0.0%wt rGO and Contact time around 80 min.*

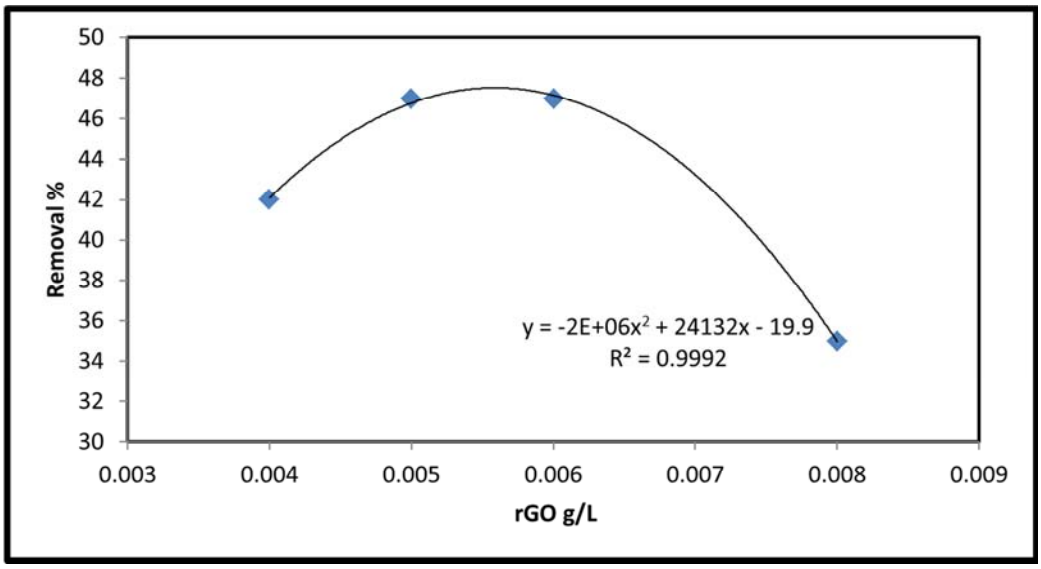

Figure 6. *Influence of rGO on photocatalytic degradation of direct red 23 in rectangular reactor. Initial concentration=50 mg L−1, ʎ=254nm, Air flowrate=10 L/min, Total catalyst concentration=3g/L and Contact time around 40 min.*

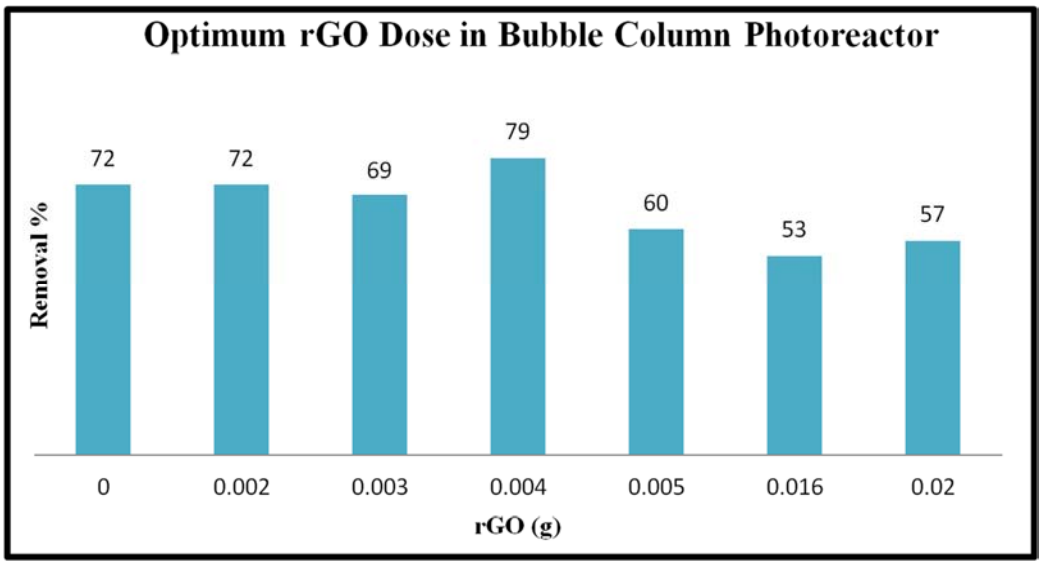

Figure 7. *Optimum rGO dose for photocatalytic degradation of direct red 23 in bubble column reactor. Initial concentration=50 mg/L, ʎ=365nm, Volume of reactor 4L, Air flowrate=15 L/min and Optimum catalyst concentration= 3g/L.*

3.4. The Effect of Initial Dye Concentration

This section illustrates the effect of initial dye concentration with range (50-200 ppm) in both rectangular and bubble column reactor respectively. Figure 8: and Figures 9: show the percentage removal after photocatalytic degradation. As the initial dye concentration increase the percentage removal of photocatalytic degradation increase. This trend can be attributed to the following reasons: Firstly, the competitive adsorption between dye molecules on the active sites on the TiO_2 surface [33]. Secondly, the molecules of the dye may inhibit light penetration; the dye molecules are not degraded immediately because the intensity of light and the catalyst amount is constant and also the light penetration is less. As the initial dye concentration increased, the solution color became more intense and the path length of the photons entering the solution was decreased, therefore the de-colorization efficiency decreases [34]. Also, the figures show that our photocatalytic system has the ability to treat high concentrations of dye solution up to 200 ppm that make the photocatalytic system suitable to be integrated with other traditional wastewater treatment processes to overcome the high operating cost which is the main restriction to reach complete mineralization. Often, photo-catalysis integrated with biological treatment in which photo-catalytic system can be used as pretreatment to convert non-biodegradable organics to biodegradable contaminates in the biological system. The same behavior was detected by Vidya Shetty K et al. He studied the photocatalytic degradation of Acid Yellow-17 by TiO_2 immobilized on Cellulose Acetate by changing the inlet dye concentration and he also found that only 5 ppm and 10 ppm dye could undergo complete degradation in 11 hours [35].

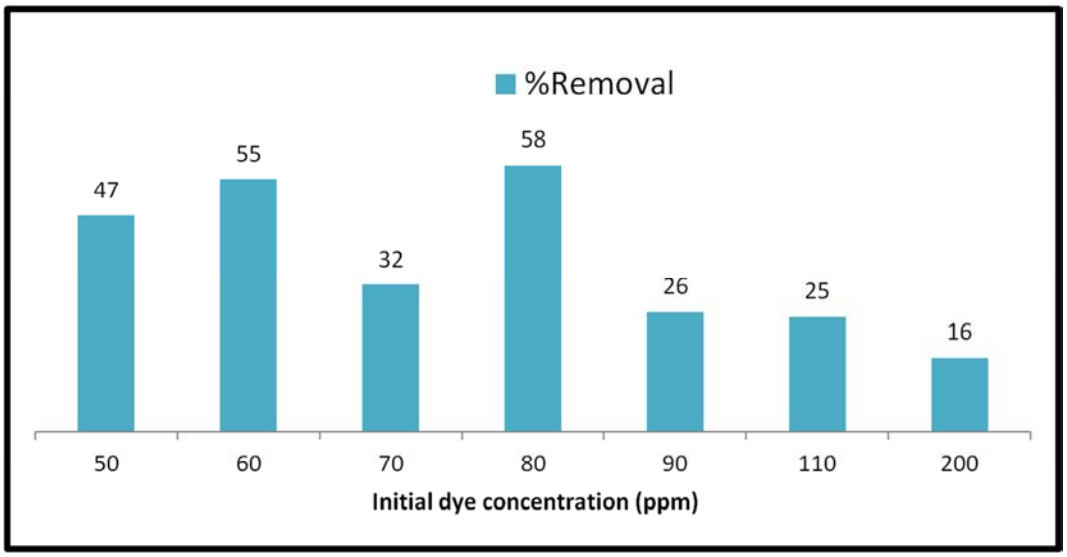

Figure 8. *Effect of initial dye concentration on the percentage removal after photocatalytic degradation in rectangular reactor. ʎ=254nm, Air flowrate=10 L/min, Optimum catalyst concentration= 3g/L and Optimum concentration of rGO= 0.005g/L.*

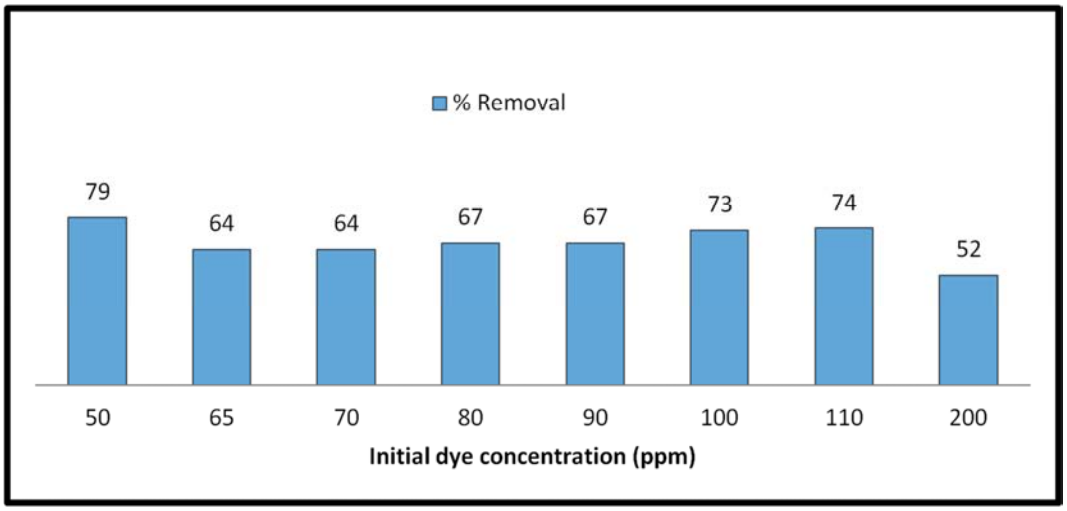

Figure 9. *Effect of initial dye concentration on the percentage removal after photocatalytic degradation in bubble column reactor. ʎ=365nm, Air flowrate=15 L/min, Optimum catalyst concentration= 3g/L and Optimum concentration of rGO= 0.001g/L.*

3.5. The Effect of Air Flowrate

Figure: 10 show the effect of air flowrate in rectangular. It is clear that increasing air flowrate lead to slight increase in the photocatalytic activity from 5 L/min up to 25 L/min. The increasing in efficiency by increasing air flowrate attributed to increasing oxygen concentration which works as oxidizing agent by trapping electrons from the conduction band of TiO_2, that lead to decrease in e^-/h^+ recombination, enhance $OH^·$ Formation and increase photocatalytic activity.

In the bubble column reactor, the effect of air flowrate can be represented in Figure: 11. As the air flowrate increase from 7.5 to 15 L/min, the photocatalytic activity increase. Further increase in air flowrate from 20 to 35 L/min causes decrease in the process efficiency. We can explain the behavior of air flowrate inside bubble column reactor according to the hydrodynamic condition. The results show presence of bubbly flow regime and transition region inside the bubble column with changing air flowrate from 7.5 L/min to 35 L/min. At low air flowrates from 7.5 to 15 L/min, bubbly flow regime is exist which characterized by a uniform bubble distribution and relatively gentle mixing is observed over the entire cross-sectional area of the column. There is practically no bubble coalescence or break-up. In this regime the efficiency of flowrate increase from 42% at 7.5 L/min to reach its maximum value 79% at 15 L/min. Further increasing in air flowrate decrease the photocatalytic degradation due to the presence of transition region from bubbly flow regime to heterogeneous flow regime; in that region, large bubbles with short contact times are formed by coalescence due to high gas throughputs. In the transition region, gas liquid interfacial area decreased and photocatalytic activity decreased from 64% at 20 L/min to be 41% at 35 L/min. The same result was obtained from Konsowa et al. and Vishnu Pareek et al. [36, 37].

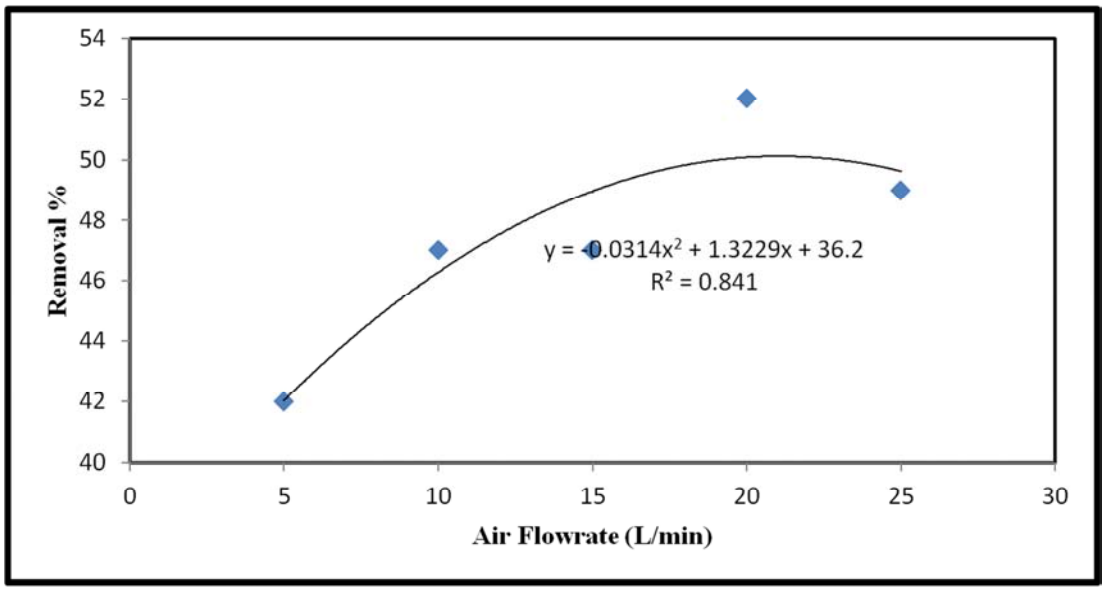

Figure 10. *Effect of Air flowrate on photocatalytic degradation in rectangular reactor. Dye concentration= 50ppm, ʎ= 254nm, Optimum catalyst concentration= 3g/L and Optimum concentration of rGO= 0.005g/L.*

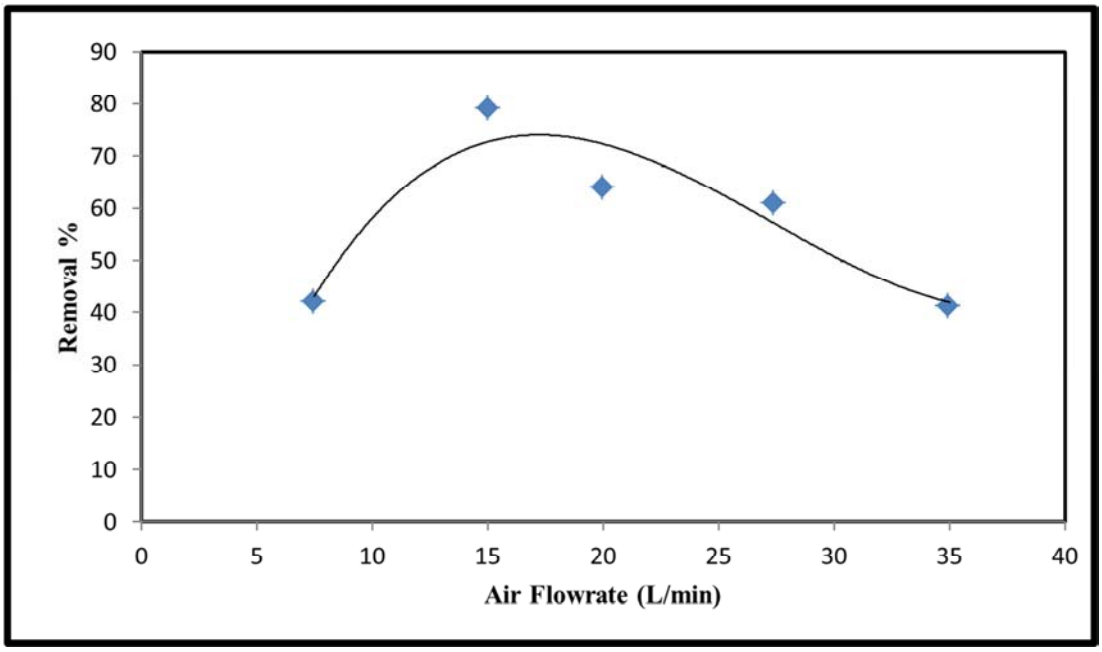

Figure 11. *Effect of Air flowrate on photocatalytic degradation in bubble column reactor. Dye concentration= 50ppm, ʎ= 365nm, Optimum catalyst concentration= 3g/L and Optimum concentration of rGO= 0.001g/L.*

3.6. The Effect of Light Wavelength

UV lamp with 254 nm & 365 nm and constant intensity 8W was used in rectangular reactor to study the effect of different wavelength on the photocatalytic degradation of direct red 23 (scarlet 4BS) dye.

As shown in figure: 12 using various wavelengths of the UV lamp has a significant effect on the photocatalytic activity. Shorter wavelength is more effective in photocatalytic degradation. The removal efficiency increased from 9% to 47% by using UV lamp with 365 & 245 nm respectively. That can be explained by the fact that electron-hole generation rate increased considerably with increasing energy of irradiation (i.e. decreasing wavelength) due to the higher densities of electron states at higher energies in TiO_2 [38].

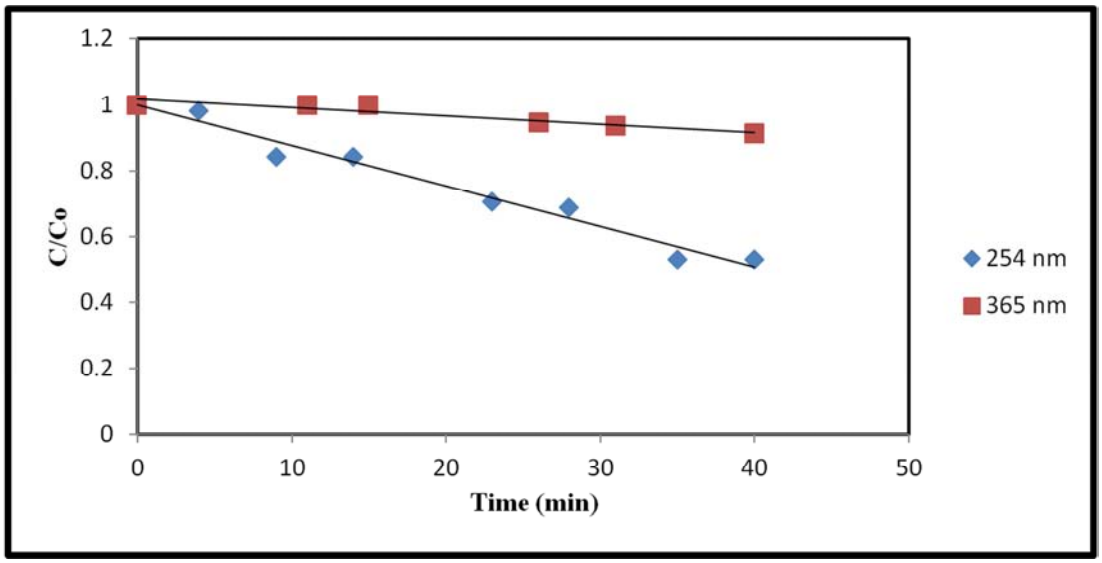

Figure 12. *Effect of Light Wavelength on photocatalytic degradation in rectangular reactor. Dye concentration= 50ppm, Air flowrate= 10L/min, Light intensity=8W, Optimum catalyst concentration= 3g/L and Optimum concentration of rGO= 0.005g/L.*

3.7. Photo-Reactor Configuration

3.7.1. Effect of Photo-Reactor Configuration on the Efficiency of Photocatalytic Degradation

One of the main objectives of this study is to investigate the effect of reactor configuration on photo-catalysis. The configuration of the photo-reactor has a great effect on the photocatalytic degradation of dye direct red 23. Slurry rectangular reactor and bubble column reactor were studied and compared. The proposed slurry reactors provide a sufficient percentage removal (%R) of azo dye whose value is controlled by different parameters.

Figure: 13 confirm the overall performance of bubble column reactor was better than rectangular reactor; the photocatalytic degradation can be enhanced from 9% to 29% at the same operating parameters for rectangular reactor and bubble column reactor respectively. This is because bubble column has excellent mass transfer characteristics, meaning high mass transfer coefficients which enhance the efficiency of the process. Behin et al studied decolorization of reactive red 33 by O3/UV in a bubble column reactor and he detected the same results [39]. However, the low efficiency can be enhanced by adjusting the operating parameters as shown in the previous sections. This comparison aims to show that efficiency of bubble column is threefold higher than rectangular reactor at the same conditions.

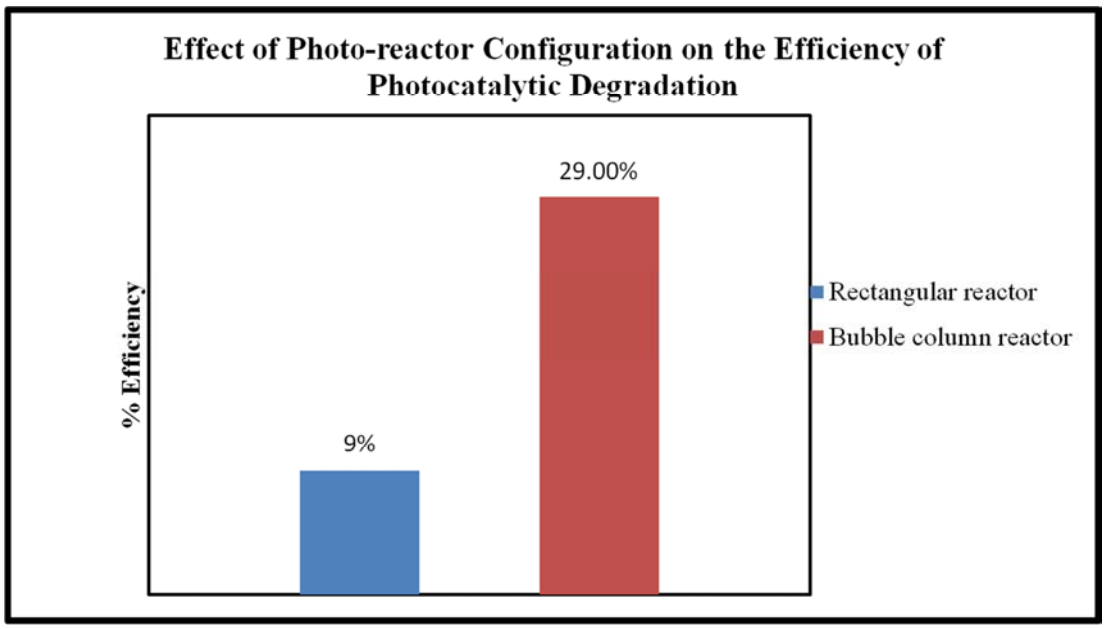

Figure 13. *Effect of Photo-reactor System on Efficiency of Photocatalytic Degradation of Direct Red 23 Dye. Dye concentration= 50ppm, λ= 365nm, Optimum catalyst concentration= 3g/L, Air flowrate= 10 L/min and Contact time= 40 min.*

3.7.2. Effect of Photo-reactor System on the Photocatalytic Degradation Efficiency of High Initial Dye Concentration

Photocatalytic degradation is demonstrated to treat low concentrations of organic pollutants. However, we used concentration up to 200 ppm to be investigated in this work. Figure: 14 show the ability of each photo-reactor systems to treat high concentrations from dye solution with high efficiency. It is clear that rectangular reactor system can treat only low concentrations with high efficiency and high concentrations with very low efficiency up to 26% for 110 ppm. However, bubble column reactor system can treat low and high concentrations with high efficiency reach to 69% for 110 ppm after only 40 min.

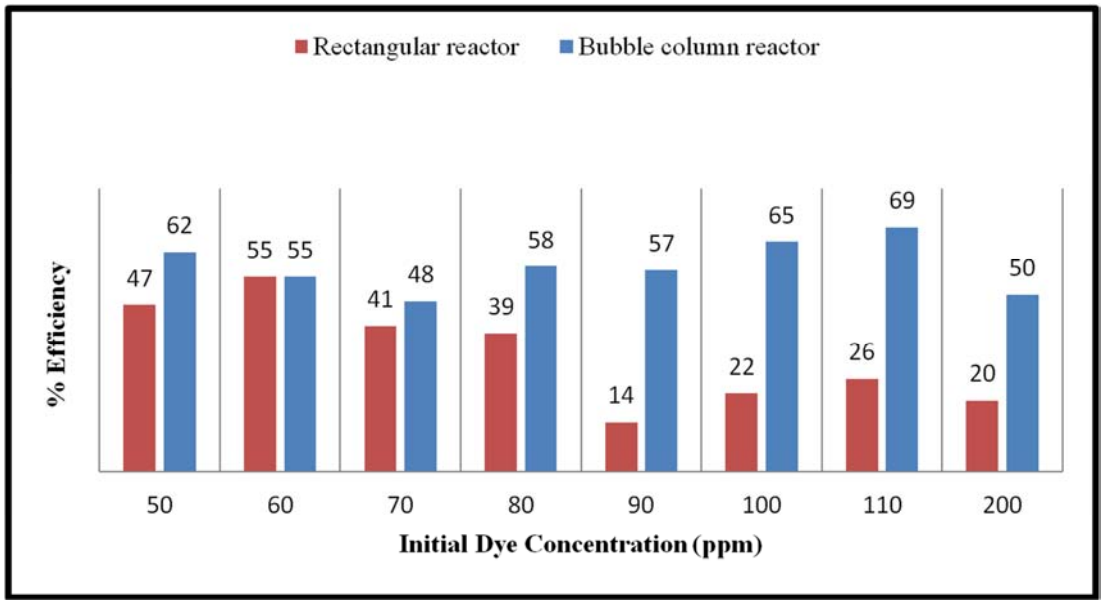

Figure 14. *Effect of Photo-reactor System on Photocatalytic Degradation Efficiency of High Initial Dye Concentrations. Optimum catalyst concentration= 3g/L, and Contact time= 40 min.*

4. Conclusions

The proposed slurry reactors provide a sufficient percentage removal (%R) of azo dye whose value is controlled by different parameters. The photo-catalysis efficiency increases by combine Anatase TiO_2 with reduced graphene oxide (rGo) by simple mixing. Adjusting operating condition and selecting suitable additives with low concentrations lead to further increasing in photocatalytic degradation.

The degradation efficiency increases with increasing the catalyst concentration up to the limiting value 3g/L in both rectangular and bubble column reactor. However, the optimum concentration of graphene was decreased fivefold in the bubble column reactor. In rectangular reactor, the process efficiency increase slightly by increasing air flowrate from (5 to 25 L/min) and increase significantly by decreasing wavelength of the irradiated lamp from 365 nm to 254 nm.

In general the performance of bubble column reactor was better than rectangular reactor because it has excellent mass transfer characteristics, meaning high mass transfer coefficients which enhance the efficiency of the process. High catalyst dose and low efficiency of rectangular reactor due to accumulation of catalyst and dye molecule in dead zones present in corners and low mixing condition. In contrast, absence of dead zones and accumulation inside bubble column and high mixing condition make it has the ability to treat high concentrations with high efficiency and low contact time.

The results show that it is not essential to obtain complete mineralization in photocatalytic process. However, the main objective is to convert non-biodegradable contaminates into biodegradable organics to integrate photocatalytic process with conventional wastewater treatment specially biological treatment to maximize the overall efficiency, reduce the operating cost of the process and make it applicable in industrial scale.

References

[1] M. R. Sohrabi, M. Ghavamiphotocatalytic Degradation Of Direct Red 23 Dye Using UV/TiO_2: Effect Of Operational Parameters, Journal Of Hazardous Materials 153 (2008) 1235–1239.

[2] N. Sobana, K. Selvam, M. Swaminathan, Optimization Of Photocatalytic Degradation Conditions Of Direct Red 23 Using Nano-Ag Doped TiO_2, Separation And Purification Technology 62 (2008) 648–653.

[3] Haidong Liao, Sol-Gel Synthesis And Photocatalytic Characterization Of Immobilized TiO_2 Films, Licentiate Thesis In Chemistry Stockholm, Sweden 2009.

[4] Bill Grote, Application of Advanced Oxidation Processes (AOP) In Water Treatment, Skillstech Australia, 2012.

[5] Pap Zsolt, Synthesis, Morpho-Structural Characterization and Environmental Application Of Titania Photocatalysts Obtained By Rapid Crystallization, Phd Thesis, University Of Szeged, Babes-Bolyai University 2011.

[6] Rowan Leary, Aidan Westwood, Carbonaceous Nanomaterials for the Enhancement of TiO_2 Photocatalysis, CARBON49 (2011) 741–772.

[7] Ying Yu, Jimmy C. Yu, Cho-Yin Chan, Yan-Ke Che, Jin-Cai Zhao, Lu Ding, Wei-Kun Ge, Po-Keung Wong, Enhancement Of Adsorption And Photocatalytic Activity of TiO_2 By Using Carbon Nanotubes For The Treatment of Azo Dye, Applied Catalysis B: Environmental 61 (2005) 1–11.

[8] Wenguang Wang, Jiaguo Yu, Quanjun Xiang, Bei Cheng, Enhanced Photocatalytic Activity Of Hierarchical Macro/Mesoporous TiO_2–Graphene Composites For Photodegradation Of Acetone In Air, Applied Catalysis B: Environmental 119– 120 (2012) 109– 116.

[9] K. S. Novoselov, A. K. Geim, S. V. Morozov, D. Jiang, Y. Zhang, S. V. Dubonos, I. V. Grigorieva, A. A. Firsov, Electric field effect in atomically thin carbon films, Science 306 (2004) 666–669.

[10] Zhai Qianqian, Bo Tang, Hu Guoxin, High Photoactive And Visible-Light Responsive Graphene/Titanate Nanotubes Photocatalysts: Preparation And Characterization, Journal Of Hazardous Materials 198 (2011) 78– 86.

[11] N. R. Khalid, E. Ahmed, Zhanglian Hong, Yuewei Zhang, M. Ahmad, Nitrogen Doped TiO2 Nanoparticles Decorated On Graphene Sheets For Photocatalysis Applications, Current Applied Physics Xxx (2012) 1-8.

[12] N. Bouazza, M. Ouzzine, M. A. Lillo-Ro ´Denas, D. Eder, A. Linares-Solano, TiO2 Nanotubes And CNT– TiO2 hybrid Materials For The Photocatalytic Oxidation of Propene at Low Concentration, Applied Catalysis B: Environmental 92 (2009) 377–383.

[13] Tayyaba Muhammad Akram, Nasir Ahmad, Irfan Ahmad Shaikh, Photocatalytic Degradation of Synthetic Textile Effluent by Modified Sol-Gel, Synthesized Mobilized and Immobilized TiO2, and Ag-doped TiO2, Pol. J. Environ. Stud. Vol. 25, No. 4 (2016), 1391-1402.

[14] Shaohua Wang, Shaoqi Zhou, Photodegradation of Methyl Orange By Photocatalyst of Cnts/P- TiO2 under Uv and Visible-Light Irradiation, Journal Of Hazardous Materials185 (2011) 77–85.

[15] Hongtao Yu, Xie Quan, Shuo Chen, Huimin Zhao, Yaobin Zhang, TiO2–Carbon Nanotube Heterojunction Arrays With A Controllable Thickness of TiO2 Layer And Their First Application In Photocatalysis, Journal Of Photochemistry And Photobiology A: Chemistry 200 (2008) 301–306.

[16] Chang Hyo Kim, Bo-Hye Kim, Kap Seung Yang, TiO2 Nanoparticles Loaded On Graphene/Carbon Composite Nanofibers By Electrospinning For Increased Photocatalysis, CARBON50 (2012) 2472–2481.

[17] Guodong Jiang, Zhifen Lin, Lihua Zhu, Yaobin Ding, Heqing Tang, Preparation And Photoelectrocatalytic Properties of Titania/Carbon Nanotube Composite Films, CARBON48 (2010) 3369–3375.

[18] Aisien Felix, Amenaghawon Andrew, Assogba Mededode, Heterogeneous Photocatalytic Degradation of Naphthalene using Periwinkle Shell Ash: Effect of Operating Variables, Kinetic and Isotherm Study, South African Journal of Chemical Engineering, vol. 19, 2014, no. 1, pp 31-45.

[19] Luisa M. Pastrana-Martínez, Sergio Morales-Torresa, Vlassis Likodimos, José L. Figueiredo, Joaquim L. Faria, Polycarpos Falaras, Adrián M. T. Silva, Advanced Nanostructured Photocatalysts Based On Reduced Graphene Oxide– TiO2 Composites For Degradation Of Diphenhydramine Pharmaceutical And Methyl Orange Dye, Applied Catalysis B: Environmental 123– 124 (2012) 241– 256.

[20] Yun Hau Ng, Akihide Iwase, Nicholas J. Bell, Akihiko Kudo, Rose Amal, Semiconductor/Reduced Graphene Oxide Nanocomposites Derived From Photocatalytic Reactions, Catalysis Today164 (2011) 353–357.

[21] Min Shi, Jianfeng Shen, Hongwei Ma, Zhiqiang Li, Xin Lu, Na Li, Mingxin Ye, Preparation Of Graphene– TiO2 composite By Hydrothermal Method From Peroxotitanium Acid And Its Photocatalytic Properties, Colloids And Surfaces A: Physicochem. Eng. Aspects Xxx (2012) Xxx– Xxx.

[22] Yulin Min, Kan Zhang, Wei Zhao, Fangcai Zheng, Youcun Chen, Yuanguang Zhang, Enhanced Chemical Interaction Between TiO2 and Graphene Oxide For Photocatalytic Decolorization Of Methylene Blue, Chemical Engineering Journal 193-194 (2012) 203–210.

[23] Bernaurdshaw Neppolian, Andrea Bruno, Claudia L. Bianchi, Muthupandian Ashokkumar, Graphene Oxide Based Pt– TiO2 photocatalyst: Ultrasound Assisted Synthesis, Characterization And Catalytic Efficiency, Ultrasonics Sonochemistry 19 (2012) 9–15.

[24] Chengyi Houa, Qinghong Zhang, Yaogang Li, Hongzhi Wang, P25–Graphene Hydrogels: Room-Temperature Synthesis And Application For Removal Of Methylene Blue From Aqueous Solution, Journal Of Hazardous Materials 205– 206 (2012) 229– 235.

[25] Thuy-Duong Nguyen-Phan, Viet Hung Pham, Eun Woo Shin, Hai-Dinh Pham, Sunwook Kim, Jin Suk Chung, Eui Jung Kim, Seung Hyun Hur, The Role Of Graphene Oxide Content On The Adsorption-Enhanced Photocatalysis Of Titanium Dioxide/Graphene Oxide Composites, Chemical Engineering Journal170 (2011) 226–232.

[26] Donglin Zhao, Guodong Sheng, Changlun Chen, Xiangke Wang, Enhanced Photocatalytic Degradation Of Methylene Blue Under Visible Irradiation On Graphene@ TiO2 Dyade Structure, Applied Catalysis B: Environmental 111– 112 (2012) 303– 308.

[27] ZHAO Huimin, SU Fang, FAN Xinfei, YU Hongtao, WU Dan, QUAN Xie, Graphene- TiO2 Composite Photocatalyst With Enhanced Photocatalytic Performance, Chin. J. Catal., 2012, 33: 777–782.

[28] Eunwoo Lee, Jin-Yong Hong, Haeyoung Kang, Jyongsik Jang, Synthesis Of TiO2 nanorod-Decorated Graphene Sheets And Their Highly Efficient Photocatalytic Activities Under Visible-Light Irradiation, Journal Of Hazardous Materials 219– 220 (2012) 13– 18.

[29] Safety Manual for The Use Of Ultra-Violet Light, School Of Chemistry, University Of Glasgow, 2013.

[30] Nanping Xu, Zaifeng Shi, Yiqun Fan, Junhang Dong, Jun Shi, And Michael Z.-C. Hu, Effects Of Particle Size Of TiO2 on Photocatalytic Degradation Of Methylene Blue In Aqueous Suspensions, Ind. Eng. Chem. Res. 1999, 38, 373-379.

[31] Jutaporn Chanathaworn, Charun Bunyakan, Wisitsree Wiyaratn, And Juntima Chungsiriporn, Photocatalytic Decolorization Of Basic Dye By TiO2 Nanoparticle In Photoreactor, Songklanakarin J. Sci. Technol. 34 (2), 203-210, Mar. - Apr. 2012.

[32] Shizhen Liu, Hongqi Sun, Shaomin Liu, Shaobin Wang, Graphene Facilitated Visible Light Photodegradation Of Methylene Blue Over Titanium Dioxide Photocatalysts, Chemical Engineering Journal 214 (2013) 298–303.

[33] Satyen Gautam, Sanjay P Kamble, Sudhir B Sawant And Vishwas G Pangarka, Photocatalytic Degradation Of 3-Nitrobenzenesulfonic Acid In Aqueous TiO2 Suspensions, J Chem Technol Biotechnol81:359–364 (2006).

[34] Jutaporn Chanathaworn, Charun Bunyakan, Wisitsree Wiyaratn And Juntima Chungsiriporn, Photocatalytic Decolorization Of Basic Dye By TiO2 Nanoparticle In Photoreactor, Songklanakarin J. Sci. Technol. 34 (2), 203-210, Mar. - Apr. 2012.

[35] Chethana Gadiyara, Bhanupriya Boruaha, Calvina Mascarenhasa And Vidya Shetty K, Immobilized Nano TiO2 For Photocatalysis Of Acid Yellow-17 Dye In Fluidized Bed Reactor, International Journal Of Current Engineering And Technology, Special Issue1 (Sept 2013) 84-87.

[36] Y. M. S. El-Shazly; S. I. M. Ibrahim; And A. H. Konsowa, Removal Of Direct Red 23 Dye By Ozonation In A Batch Bubble Column Reactor, ADEST International Conference (2010).

[37] Yash Boyjoo, Ming Ang, And Vishnu Pareek, Photocatalytic Treatment Of Shower Water Using A Pilot Scale Reactor, Hindawi Publishing Corporation, International Journal Of Photoenergy, Volume 2012, Article ID 57891.

[38] K. Kočí, K. Zatloukalová, L. Obalová, S. Krejčíková, Z. Lacný, L. Čapek, A. Hospodková, O. Šolcová, Wavelength Effect On Photocatalytic Reduction Of CO2 By Ag/ TiO2 catalyst, Chin. J. Catal., 2011, 32: 812–815.

[39] Jamshid Behin, Negin Farhadian, Response surface methodology and artificial neural network modeling of reactive red 33 decolorization by O3/UV in a bubble column reactor, Advances in Environmental Technology 1 (2016) 33-44.